Search for Higher Twist Effects in the Neutron Spin Structure Function $g_2^n(x,Q^2)$

T. Averett (co-spokesperson), B. Filippone, E. Hughes, S. Jensen, C. Jones, R. McKeown, D. Pripstein

California Institute of Technology, Pasadena, CA 91125

J.P. Chen, K. de Jager, J. Gomez, O. Hansen, J. LeRose, M. Liang, R. Michaels, S. Nanda, P. Rutt, A. Saha, B. Wojtsekhowski

TJNAF, Hall A, Newport News, VA 23606

B. Anderson, R. Madey, D.M. Manley, G.G. Petratos, J. Watson

Kent State University, Kent, OH 44242

D. Dale, T. Gorringe, W. Korsch (co-spokesperson), M. Kovash, V. Zeps

University of Kentucky, Lexington, KY 40506

T. Black, H. Gao, W. Xu

Massachusetts Institute of Technology, Cambridge, MA 02139

G.D. Cates, G.S. Corrado, B. Humensky, I. Kominis, K. Kumar, T. Pavlin

Princeton University, Princeton, NJ 08544

C. Glashausser, R. Gilman, J. McIntyre, R.D. Ransome

Rutgers University, Rutgers, NJ 08855

R. Holmes, J. McCracken, P.A. Souder

Syracuse University, Syracuse, NY 13210

L. Auerbach, Z.-E. Meziani, K. Slifer

Temple University, Philadelphia, PA 19122

M. Pitt

Virginia Polytechnic Institute, Blacksburg, VA 24061

M. Finn

The College of William and Mary, Williamsburg, VA 23185

Abstract

We propose to make the first high precision measurement of the neutron spin structure funtion g_2^n in the kinematic range $0.14 < x < 0.22$ and $0.6 < Q^2 < 1.5$ (GeV/c)^2. This structure function has a unique sensitivity to higher twist effects and quark-gluon correlations which are suppressed in typical deep inelastic scattering measurements at higher Q^2's. The ability to achieve errors which are more than an order of magnitude smaller than the current world average, along with the lower Q^2 range available at TJNAF, provide us with the opportunity to quantify these higher twist effects which was not available in previous measurements. The structure function will be determined by measuring the inclusive electron asymmetry for polarized electrons on a polarized ^{3}He gas target currently under construction. We are requesting $15\mu A$ of polarized beam for a total of 680 hours in Hall A and the usual laboratory support for the beam polarimetry, experimental setup, and target installation.

I. Physics Motivation

For the past 20 years, there has been a large effort undertaken in the physics community to understand the spin structure of the nucleon. Most of this effort has centered around the measurement of the polarized deep-inelastic (DIS) structure function $g_1(x, Q^2)$ for the proton and neutron [1, 2, 3, 4, 5, 6, 7, 8]. Precise measurements of this quantity have allowed us to test the fundamental Bjorken sum rule, and within the quark-parton model, to extract the contribution of the quarks to the nucleon spin. For the most part, the quark-parton model provides a reasonable interpretation of g_1, with pQCD effects to account for the finite Q^2 of the measurements. However, in order to have a complete understanding of the nucleon spin structure, it is necessary to understand the role of the quark-gluon correlations. In the case of spin-dependent DIS, there exists another structure funtion, $g_2(x, Q^2)$, which has no simple quark-parton model interpretation due to its unique sensitivity to the quark-gluon interactions within the nucleon. Measuring this structure function gives us the opportunity to look for so-called higher twist effects in the nucleon structure which are supressed by $1/Q^2$ or more in g_1.

To study the spin structure of the nucleon in inclusive electron-nucleon DIS, we require that both the incident lepton and the target nucleon be polarized. Fig. 1 shows a longitudinally polarized incident electron with 3-momentum $\vec{k}$ and energy E. The target nucleon is at rest in the lab frame with polarization vector $\vec{p}$ at an angle of α with respect to the incident electron direction. The outgoing electron is detected at an angle θ with respect to the incident electron direction with 3-momentum $\vec{k'}$ and energy E'. The cross section difference between a target polarized along α and $\alpha + \pi$ is

$$\frac{d^3(\sigma(\alpha) - \sigma(\alpha+\pi))}{dx\ dy\ d\phi} = \frac{e^4}{4\pi^2 Q^2}\left\{cos(\alpha)\left\{(1 - \frac{y}{2} - \frac{y^2}{4}\gamma^2)\ g_1(x,Q^2) - \frac{y}{2}\gamma^2 g_2(x,Q^2)\right\} - \right.$$
$$\left. sin(\alpha)cos(\phi)\sqrt{\gamma^2(1 - y - \frac{y^2}{4}\gamma^2)}\left\{\frac{y}{2}\ g_1(x,Q^2) + g_2(x,Q^2)\right\}\right\}\ . \qquad (1)$$

Here $y = \nu/E$ and $\gamma = \sqrt{Q^2}/\nu$ where $\nu = E - E'$, $Q^2 = 2EE'(1 - cos\theta)$ is the four-momentum transfer squared, $x = Q^2/2M\nu$ is the Bjorken scaling variable, and M is the mass of the nucleon.

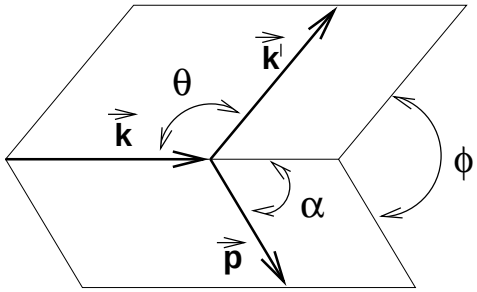

Figure 1: Definition of scattering and polarization angles.

Eq. 1 contains the two spin structure functions $g_1(x,Q^2)$ and $g_2(x,Q^2)$. The equation is valid for both protons and neutrons, although the structure functions are not necessarily the same for the two types of nucleons. By measuring the scattering asymmetries for different beam and target polarization configurations, (e.g. ϕ=0, and the target polarization vector parallel (α=0), or perpendicular (α=$\pi/2$) to the beam polarization), both of the structure functions can be extracted. As mentioned above, most of the effort up to now has gone into precision measurements of the structure functions $g_1^p(x,Q^2)$ and $g_1^n(x,Q^2)$ in order to test the Bjorken sum rule and to measure the quark contribution to the nucleon spin. However, very little information is available on the other spin structure function $g_2(x,Q^2)$. This structure function is of special interest, because of its unique sensitivity to quark-gluon correlations. Ignoring quark mass effects, $g_2(x,Q^2)$ can be decomposed into the sum of two terms:

$$g_2(x,Q^2) \;=\; g_2^{WW}(x,Q^2) + \bar{g}_2(x,Q^2)\;. \tag{2}$$

This decomposition was first proposed by Wandzura and Wilczek (WW) [9]. Generally, the moments of the spin structure functions in DIS can be expressed in terms of hadronic matrix elements with increasing twist τ in the operator product expansion (OPE). The lowest, and therefore leading, twist contribution is twist-2, with higher twist effects suppressed by powers of $1/|Q|^{\tau-2}$. In the above expression, g_2^{WW} is purely twist-2 and can be expressed in terms of $g_1(x,Q^2)$ as follows:

$$g_2^{WW} \;=\; -g_1(x,Q^2) \;+\; \int_x^1 \frac{g_1(y,Q^2)}{y} dy\;. \tag{3}$$

The second term, $\bar{g}_2(x,Q^2)$, comes from twist-3 and higher operators, and is sensitive to quark-gluon interactions in the nucleon. We would like to mention that this term can also have contributions from a twist-3 quark-mass-dependent operator, if quark masses cannot be neglected [10]. These various twist-3 contributions do not exist for g_1, but appear in the expression for g_2 at leading order, allowing us to look for higher twist effects directly by measuring g_2 and subtracting the twist-2 contribution using the g_2^{WW} expression [11]. Twist-4 and higher contributions to g_1 and g_2 are supressed by additional powers of $1/Q$.

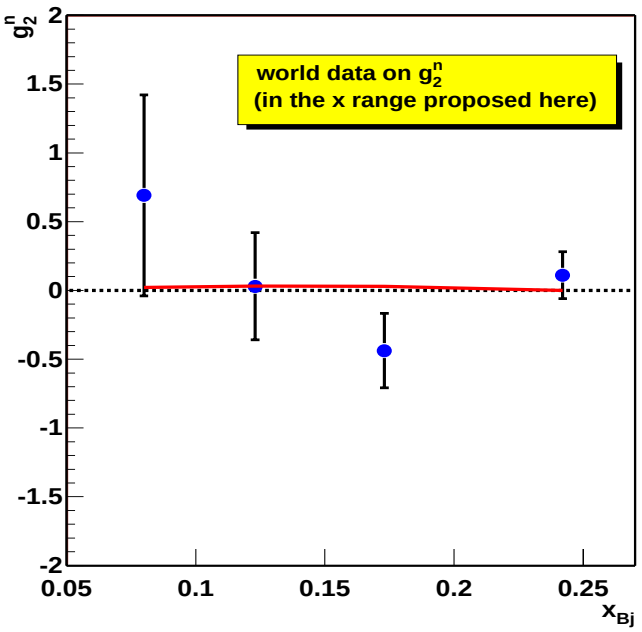

Figure 2: Combined data from SLAC experiments E142, E143, and E154 for the structure function $g_2^n(x,Q^2)$ of the neutron. The solid line is the twist-2 g_2^{WW} prediction.

Because of the $1/Q$ dependence of the higher twist contributions mentioned above, typical DIS measurements of g_2 at $Q^2 \sim 5$ (GeV/c)^2 have limited sensitivity to these effects. Currently, the best data for g_2 are the relatively low statistics measurements for the proton, deuteron and neutron made by the E142, E143 and E154 collaborations at SLAC in the kinematic range $0.03<x<0.8$ and $1.3<Q^2<17.0$(GeV/c)^2 [12, 13, 14]. Fig. 2 shows the results for g_2 for the neutron for all SLAC experiments combined in the x range of interest at TJNAF. Also shown is the twist-2 g_2^{WW} prediction which is barely distinguishable from zero on this scale. These data clearly show that significantly better statistics are needed to make a conclusive statement about higher twist contributions as well as x and Q^2 dependence to g_2. We therefore propose to perform a precision measurment of g_2^n at x values between 0.14 and 0.22 covering a Q^2 range between 0.6 and 1.5 GeV^2/c^2. For each x value, data will be taken at two different values of Q^2 to look for Q^2 dependence in the higher twist contributions. We propose to do the experiment in Hall A using the polarized ^{3}He target currently being built for several approved experiments [15] in Hall A. Previous spin structure function measurements have not seen any effects from the nuclear medium of the target material and

are not expected to significantly contribute to the extraction of higher twist effects [16, 17].

Also note that there is a measurement of g_2 planned at SLAC on the proton and deuteron at a beam energy of 29 GeV [18]. However, the neutron results extracted from that experiment will have only two overlapping data points with this proposal, and will have errors which are approximately 10 times larger, and at significantly higher Q^2.

The precision of this proposed measurement, along with the lower average Q^2 than previous measurements, will provide a unique opportunity to seach for higher twist contributions to the nucleon spin structure.

II. Measurement of $g_2^n(x,Q^2)$

To separate the spin structure functions g_1^n and g_2^n, we will measure the scattering asymmetries with the target polarization both parallel ($A_\parallel$) and perpendicular ($A_\perp$) to the incident electron helicity (electrons are polarized parallel or anti-parallel to the beam direction).

The structure functions g_1 and g_2 can be expressed in terms of these measured asymmetries as follows [23]:

$$g_1(x,Q^2) = \frac{F_1(x,Q^2)}{D}\left[A_\parallel + \tan\left(\theta/2\right) A_\perp\right] \tag{4}$$

$$g_2(x,Q^2) = \frac{F_1(x,Q^2)}{D}\frac{y}{2\sin\theta}\left[\frac{E+E'\cos\theta}{E'}A_\perp - \sin\theta A_\parallel\right] \tag{5}$$

where θ is the scattering angle, $D = (1-\epsilon)(2-y)/y[1+\epsilon R(x,Q^2)]$, $\epsilon = 1/[1+2(1+1/\gamma^2)\tan^2(\theta/2)]$, and $\gamma^2 = Q^2/\nu^2$.

$F_1(x,Q^2)$ is a spin independent structure function and is related to the unpolarized structure function $F_2(x,Q^2)$, and $R(x,Q^2)$, the ratio of longitudinal to transverse virtual photoabsorption cross sections as follows

$$F_1(x,Q^2) = F_2(x,Q^2)(1+\gamma^2)/2x(1+R(x,Q^2)). \tag{6}$$

Using our measured asymmetries, along with previously measured data for F_2 and R, we can obtain the two spin structure functions.

III. Count Rate Estimates and Backgrounds

In order to perform a high precision measurement of g_2^n at several different values x and Q^2 we plan to use the same polarized ^{3}He target currently under construction for several experiments approved for Hall A (target details will be given in a later section). The ^{3}He atoms will be contained in a 40 cm long glass cell at a density of approximately 2.5×10^{22} atoms/cm^3. The nuclei are polarized via spin exchange collisions with optically pumped rubidium. In addition to the ^{3}He, the target cell contains about 100 torr of nitrogen (1.4×10^{19} atoms/cm^3) and rubidium atoms with a density of about 6×10^{14} atoms/cm^3. These additional atoms will dilute the measured asymmetry. Therefore the measured asymmetry can be expressed as follows:

$$A_{meas} \;=\; P_e \cdot P_n \cdot f \cdot A_{phys} \quad , \tag{7}$$

with P_e being the electron polarization, we assume 80%, and P_n is the neutron polarization. The ^{3}He polarization is expected to be about 45%, and the neutron itself carries about 87% of the polarization of the ^{3}He. f is a dilution factor, which corrects for scattering from nuclei other than ^{3}He and also for the fact that the ^{3}He is itself composed of 2 protons and a neutron. In order to estimate the statistical uncertainties in the asymmetries, we need to calculate the inclusive rates for the lepton-nucleon scattering process. For the $F_2(x,Q^2)$ structure function, we use a fit to the proton and the neutron (extracted from deuteron data) as performed by the NMC collaboration [22]. Fig. 3 shows a compilation of the data on F_2 of the proton [24]. The figure shows that F_2 has been measured down to Q^2 values well below 1 GeV^2/c^2 in the x region which is of interest for our experiment ($0.1<x<0.3$). Data of similar quality exist for the deuteron and therefore F_2 for the neutron is also known to high precision.

The structure function F_1 was calculated using a fit to $R(x,Q^2)$ (the ratio of the longitudinal to transverse virtual photon absorption cross section) as given in Whitlow *et al.* [21]. The fit covers a range in x from 0.1 to 0.9 and a Q^2 range from 0.6 to 20 GeV^2/c^2. So, F_1 and F_2, and therefore the electron-nucleon cross section is well known in the kinematic range proposed here. This experiment will use both of the Hall A spectrometers simultaneously as independent electron spectrometers. For the count rate estimates we made the following assumptions for the Hall-A spectrometers:

$\delta p/p = \pm 4.5\%$, target length: 8 cm, solid angle: 6.4 msr, online pion rejection 50:1.

We expect that the maximum allowable data rate for each spectrometer is 2.0 kHz and assume that the online pion rate can be reduced by factor of 50 by using a particle identifaction trigger (PID). However, we do not expect to be rate limited in this experiment and should be able to safely run without any online pion rejection if desired. For the of-

Figure 3: The structure function $F_2^p(x,Q^2)$.

fline analysis, pion rejection is expected to be 50,000:1 for the electron spectrometer and 1000:1 for the hadron spectrometer. Additionally, a shower calorimeter is being constructed for the hadron spectrometer to increase the pion rejection to 10,000:1. Also note that the spectrometers see only approximately 8 cm in the middle of the target cell and will not be sensitive to electrons produced in the unpolarized glass target windows. However, to help reduce any possible backgrounds associated with the glass, collimators will be placed near the target to further shield them from the windows. For this experiment, we assume that we will be limited to a maximum beam current of $15\mu A$ due to target depolarization effects. In this case, the spectrometers will run well below the 2 kHz limit. If, however, the target will allow for higher beam currents, we will be able to take advantage of the increased rate.

In order to get a reasonable estimate for the running time needed, we estimated the size of the expected asymmetries in the following way. First we used a fit to the g_1^n data points obtained in the E154 experiment [8]. Note that these data were taken at an average Q^2 value of about 5 (GeV/c)^2 which is significantly higher than the Q^2 proposed here. The data were evolved to a Q^2 of 1.0 (GeV/c)^2 assuming g_1/F_1 to be independent of Q^2. From this evolved g_1, values for g_2^{nWW} (twist-2 only) at $Q^2 = 1.0$ (GeV/c)^2 were calculated using Eq. 3. Using these values for g_1 and g_2, values for the asymmetries were obtained. Therefore, the asymmetries as well as the values for g_2^n shown below are only meant to indicate an approximate size for the expected asymmetries. Table 1 summarizes the proposed kinematic settings, Table 2 shows the the expected rates together with the requested running time, and Tables 3a and 3b show the expetecd physics asymmetries and expected values of g_1^n and g_2^n, respectively, together with the predicted statistical accuracy.

III.1. Count Rate Estimates and Backgrounds

TABLE 1 Proposed kinematics for studying the sensitivity of g_2^n to higher twist contributions. Data will be taken using both spectrometers simultaneously as independent electron spectrometers. The settings for each spectrometer are listed separately. The scattering angle θ_e and the energy E' of the scattered electron correspond to the central value of the spectrometer. The invariant mass is $W > 2$ GeV/c^2 for all points to ensure DIS kinematics.

kinematic setting	E [GeV]	I [μA]	spectrometer	E′ [GeV]	θ [deg]
1	4	15	electron	1.69	17
			hadron	1.85	17
2	4	15	electron	1.69	20
			hadron	1.87	20
3	6	15	electron	1.84	18
			hadron	2.04	18
4	6	15	electron	2.24	18
			hadron	2.47	18

TABLE 2 Expected particle rates and running times. The pion rate estimates assume a factor of 50 in the PID trigger. Note that the total rates in each spectrometer are well below the 2kHz limit for each spectrometer setting.

kinematic setting	t_{par} [hrs]	t_{perp} [hrs]	e^- rate [Hz]	π^- rate [Hz]	total rate with PID [Hz]
1	6	65	250	960	270
			290	740	300
2	6	55	120	460	130
			130	310	140
3	24	305	70	825	90
			80	570	90
4	11	125	80	380	90
			90	220	90
total	47	550			

TABLE 3a Estimated physics asymmetries and expected statistical errors. The asymmetry estimates are based on existing SLAC data evolved to $Q^2 = 1.0$ (GeV/c)^2.

kinematic setting	x	Q^2 [(GeV/c)^2]	A_{par}	ΔA_{par}^{stat}	A_{perp}	ΔA_{perp}^{stat}
1	0.14	0.60	$-6.19\cdot10^{-2}$	$5.81\cdot10^{-3}$	$-1.50\cdot10^{-3}$	$1.76\cdot10^{-3}$
	0.16	0.65	$-5.70\cdot10^{-2}$	$5.53\cdot10^{-3}$	$-0.24\cdot10^{-3}$	$1.68\cdot10^{-3}$
2	0.19	0.83	$-6.09\cdot10^{-2}$	$8.77\cdot10^{-3}$	$0.34\cdot10^{-3}$	$2.90\cdot10^{-3}$
	0.22	0.91	$-5.66\cdot10^{-2}$	$8.52\cdot10^{-3}$	$2.07\cdot10^{-3}$	$2.81\cdot10^{-3}$
3	0.14	1.09	$-7.00\cdot10^{-2}$	$5.54\cdot10^{-3}$	$-1.92\cdot10^{-3}$	$1.56\cdot10^{-3}$
	0.16	1.21	$-6.71\cdot10^{-2}$	$5.41\cdot10^{-3}$	$-1.09\cdot10^{-3}$	$1.52\cdot10^{-3}$
4	0.19	1.33	$-6.45\cdot10^{-2}$	$7.85\cdot10^{-3}$	$-0.15\cdot10^{-3}$	$2.33\cdot10^{-3}$
	0.22	1.46	$-6.18\cdot10^{-2}$	$7.75\cdot10^{-3}$	$1.07\cdot10^{-3}$	$2.30\cdot10^{-3}$

TABLE 3b Estimated statistical uncertainties in the spin structure functions. The structure functions estimates are based on existing SLAC data evolved to $Q^2 = 1.0$ (GeV/c)^2.

kinematic setting	x	Q^2 [(GeV/c)^2]	g_1^n	Δg_1^n	g_2^n	Δg_2^n
1	0.14	0.60	$-7.85\cdot10^{-2}$	$7.35\cdot10^{-3}$	$1.64\cdot10^{-2}$	$7.74\cdot10^{-3}$
	0.16	0.65	$-6.69\cdot10^{-2}$	$6.49\cdot10^{-3}$	$1.73\cdot10^{-2}$	$6.01\cdot10^{-3}$
2	0.19	0.83	$-5.64\cdot10^{-2}$	$8.15\cdot10^{-3}$	$1.73\cdot10^{-2}$	$7.98\cdot10^{-3}$
	0.22	0.91	$-4.59\cdot10^{-2}$	$6.96\cdot10^{-3}$	$1.65\cdot10^{-2}$	$5.90\cdot10^{-3}$
3	0.14	1.09	$-7.70\cdot10^{-2}$	$6.08\cdot10^{-3}$	$1.66\cdot10^{-2}$	$8.39\cdot10^{-3}$
	0.16	1.21	$-6.61\cdot10^{-2}$	$5.32\cdot10^{-3}$	$1.73\cdot10^{-2}$	$6.50\cdot10^{-3}$
4	0.19	1.33	$-5.67\cdot10^{-2}$	$6.90\cdot10^{-3}$	$1.73\cdot10^{-2}$	$7.90\cdot10^{-3}$
	0.22	1.46	$-4.73\cdot10^{-2}$	$5.95\cdot10^{-3}$	$1.67\cdot10^{-2}$	$6.00\cdot10^{-3}$

The uncertainties in Tables 3a and 3b are statistical only.

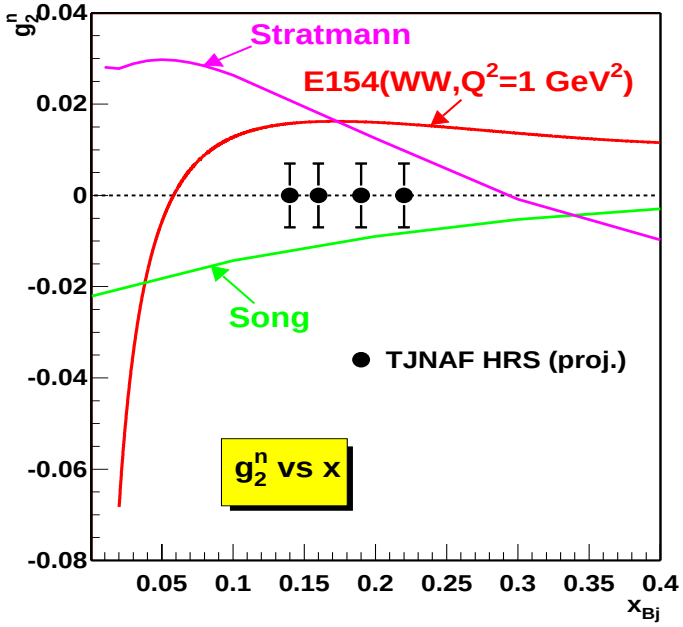

Figure 4: Projected errors on $g_2^n(x,Q^2)$. The curve labeled E154 (WW, Q^2=1) is the twist-2 WW part of g_2^n evaluated from a fit to the E154 g_1^n data. For this purpose g_1^n was evolved to a Q^2 of 1 GeV^2/c^2 assuming g_1/F_1 is independent of Q^2. Note: we will measure two data points with different Q^2 for each value of x. So only half the number of data points is shown.

Fig. 4 shows the projected (statistical) error bars for the proposed experiment. The figure includes two predictions of g_2^n at $Q^2 = 1.0$ (GeV/c)^2 together with the twist-2 part of g_2^n as extracted from a fit to the E154 g_1^n data and evolved to a Q^2 of 1.0 (GeV/c)^2 assuming g_1/F_1 is independent of Q^2. The two theoretical curves are model predictions using MIT bag model calculations. The expected errors shown in this figure are to be compared with the existing world data shown in Fig. 2 where the errors are roughly a factor of 25 or more larger, with limited kinematic coverage.

Fig. 5 shows the existing data on $g_1^n(x,Q^2)$ in the x range from 0.1 to 0.35. Our projected (statistical) error bars are comparable to the symbol size on this scale.

In order to study the effect of higher twist contributions to g_2, a precision measurement of g_1^n is necessary as well. As mentioned above, there are no twist-3 contributions to $g_1^n(x,Q^2)$ and twist-4 contributions are supressed by $1/Q^2$ relative to the leading twist-2 term. A precise measurement of g_1^n allows us to compare our measured values with a next-to-leading

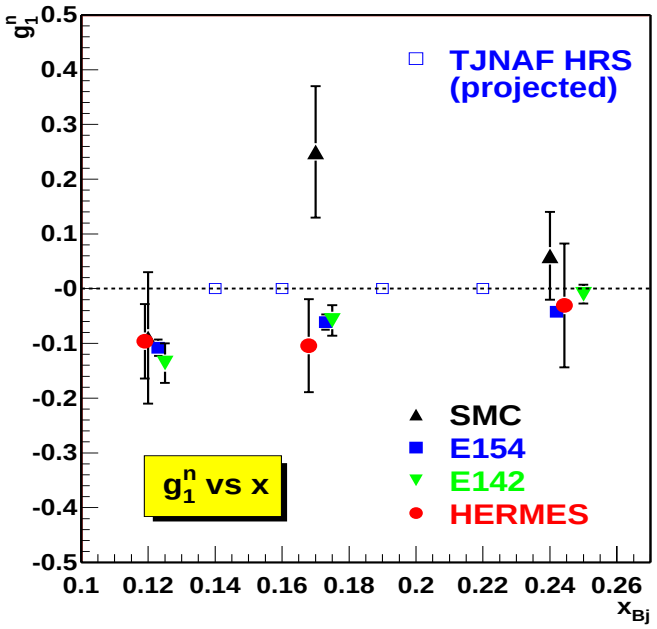

Figure 5: Projected errors on $g_1^n(x,Q^2)$ for the proposed experiment. The size of the error bars for this measurement are comparable to the symbol size. Note: we will measure two data points with different Q^2 for each value of x. So only half the number of data points is shown.

order Q^2 evolution of existing g_1^n data (e.g. see reference [27]). Further, we will use the Q^2 evolved g_1^n data to determine the twist-2 (WW) part of $g_2^n(x,Q^2)$. Any deviation from the twist-2 expectation is then expected to be a result of higher twist effects. Also note that by measuring g_1 at two different Q^2 values for each x, we will have an additional handle on the QCD and higher twist evolution in this structure function.

We plan to use the code POLRAD [28] to correct for radiative effects. This program was specifically developed for radiative corrections for DIS spin structure function measurements, and has been used extensively in experiments of this nature.

The beam polarization will be measured using the standard Hall A Moller polarimeter. We expect to measure the beam and target polarizations with relative uncertainties of 5% or better. These will be the major contributions to our systematic error. Adding these errors in quadrature gives a relative systematic error of about 7% , this is small compared to the expected statistical error.

IV. Charged Particle Backgrounds

Here we try to give an estimate of the expected rates and asymmetries coming from the charged particle backgrounds. The two dominant backgrounds are expected to be pions, and electrons produced in charge symmetric processes. We estimate in the worst case that the (π/e^-) ratio is about 1.2×10^{-3} (for E = 6 GeV and x = 0.15), assuming the offline pion rejection is 10,000:1. This background is quite small and will only contribute significantly if the pions have a relatively large asymmetry. However, most of the pions will be produced via photons produced in the upstream glass target window which is not polarized, and the asymmetry is therefore not expected to be large. Finally, note that our data stream will contain a large sample of pions, and will allow us to directly measure the backgound and asymmetry from the pions and make a correction to the electron data.

The other possible background is from electrons produced in charge symmetric decays of pions. We estimate in the worst case that the (e^+/e^-) ratio is less than 0.01. Again, this process is expected to have no asymmetry for the same reason mentioned above. However, beam time at each kinematic setting will be used to measure this backgroud by reversing the magnetic fields of the spectrometers and measuring the companion positrons from the pair production.

In general the measured asymmetry can be expressed in the following way:

$$A_{e^-} = \frac{1}{1 - e^+/e^-} \left[\frac{A_{meas} - (\pi/e^-)A_\pi}{1 - \pi/e^-} - (e^+/e^-)A_{e^+} \right] \tag{8}$$

The ratios (π/e^-) and (e^+/e^-) denote the pion and positron rates normalized to the expected electron rates. A_π and A_{e^+} are the pion and positron asymmetries. A_{meas} is the asymmetry we calculate directly from counts in the spectrometer . Then we apply polarization, dilution, and radiative corrections to A_{e^-} to get the overall physics asymmetry.

V. The Polarized ^{3}He Target

The polarized target will be based on the principle of spin exchange between optically pumped alkali-metal vapor and noble-gas nuclei [29, 30, 31]). The design will be similar in many ways to that used in E142, an experiment at SLAC to measure the spin dependent structure function of the neutron [4]. A central feature of the target will be sealed glass target cells, which will contain a ^{3}He pressure of about 10 atmospheres. As indicated in Fig. 6, the cells will have two chambers, an upper chamber in which the spin exchange takes place, and a lower chamber, through which the electron beam will pass. In order to maintain the appropriate number density of alkali-metal (which will probably be Rb) the upper chamber will be kept at a temperature of 170–200°C using an oven constructed of the high temperature plastic Torlon. With a density of 2.5×10^{20} atoms/cm^3, and a lower cell length of 40 cm, the target thickness will be 1.0×10^{22}atoms/cm^2.

Note that the target is currently being constructed for several experiments approved for Hall A at TJNAF. We are planning to use this target for our experiment in Hall A without any major upgrades or changes. We describe below in greater detail some features of the target.

V.1 Operating Principles

The time evolution of the ^{3}He polarization can be calculated from a simple analysis of spin-exchange and ^{3}He nuclear relaxation rates [32]. Assuming the ^{3}He polarization $\mathrm{P_{^3He}} = 0$ at $t = 0$,

$$\mathrm{P_{^3He}(t)} = \langle \mathrm{P_{Rb}} \rangle \left(\frac{\gamma_{\mathrm{SE}}}{\gamma_{\mathrm{SE}} + \Gamma_{\mathrm{R}}} \right) \left(1 - \mathrm{e}^{-(\gamma_{\mathrm{SE}} + \Gamma_{\mathrm{R}})\mathrm{t}} \right), \tag{9}$$

where γ_{SE} is the spin-exchange rate per ^{3}He atom between the Rb and ^{3}He, Γ_{R} is the relaxation rate of the ^{3}He nuclear polarization through all channels other than spin exchange with Rb, and $\langle \mathrm{P_{Rb}} \rangle$ is the average polarization of a Rb atom. Likewise, if the optical pumping is turned off at $t = 0$ with $\mathrm{P_{^3He}} = \mathrm{P_0}$, the ^{3}He nuclear polarization will decay according to

$$\mathrm{P_{^3He}(t)} = \mathrm{P_0 e}^{-(\gamma_{\mathrm{SE}} + \Gamma_{\mathrm{R}})\mathrm{t}}. \tag{10}$$

The spin exchange rate γ_{SE} is defined by

$$\gamma_{\mathrm{SE}} \equiv \langle \sigma_{SE} v \rangle [Rb]_A \tag{11}$$

where, $\langle \sigma_{\mathrm{SE}}\ v \rangle = 1.2 \times 10^{-19}$ cm^3/sec is the velocity-averaged spin-exchange cross section for Rb–^{3}He collisions([32, 33, 34]) and $[\mathrm{Rb}]_{\mathrm{A}}$ is the average Rb number density seen by a ^{3}He atom. Our target will be designed to operate with $1/\gamma_{\mathrm{SE}} = 8$ hours. ¿From Eq. (9) it is clear that there are two things we can do to get the best possible ^{3}He polarization

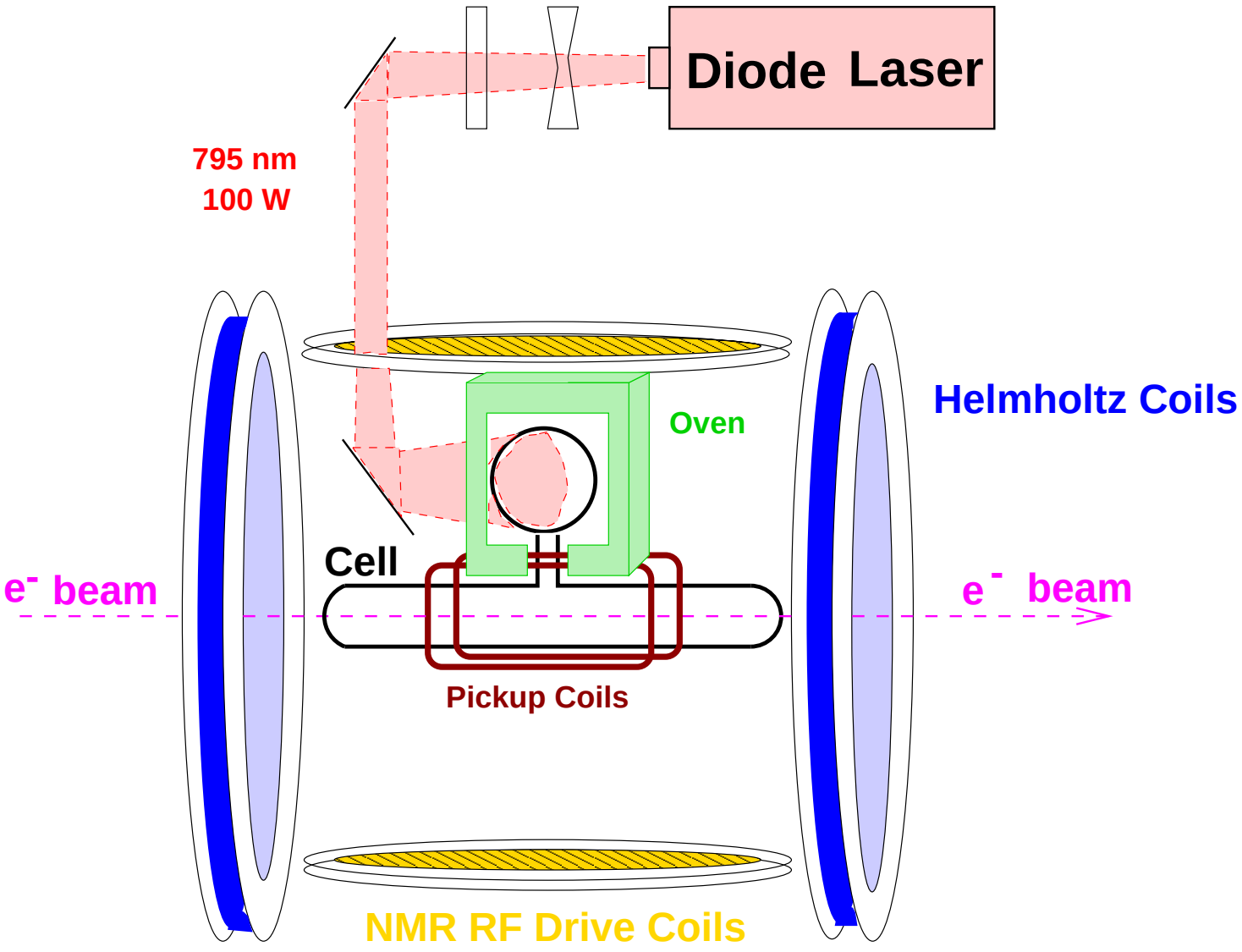

Figure 6: Schematic diagram of the polarized ^{3}He target. Note that an additional set of Helmholtz coils exist for transverse polarization, but are not shown here.

— maximize $\gamma_{\rm SE}$ and minimize $\Gamma_{\rm R}$. But from Eq. (11) it is also clear that maximizing $\gamma_{\rm SE}$ means increasing the alkali-metal number density, which in turn means more laser power. The number of photons needed per second must compensate for the spin relaxation of Rb spins. In order to achieve $1/\gamma_{\rm SE} = 8$ hours, we will require about 24 Watts of usable laser light at a wavelength of 795 nm. We will say more about the source of laser light below.

The rate at which polarization is lost, which is characterized by $\Gamma_{\rm R}$, will have four principle contributions. An average electron beam current of about 15 μA will result in a depolarization rate of $\Gamma_{\rm beam} = 1/30$ hours [35]. Judging from experience at SLAC, we can produce target cells with an intrinsic rate of $\Gamma_{\rm cell} = 1/50$ hours. This has two contributions, relaxation that occurs during collisions of ^{3}He atoms due to dipole-dipole interactions [36], and relaxation that is presumably due largely to the interaction of the ^{3}He atoms with the walls. Finally, relaxation due to magnetic field inhomogeneities can probably be held to about $\Gamma_{\nabla B} = 1/100$ hours [37]. Collectively, under operating conditions, we would thus expect

$$\Gamma_{\rm R} = \Gamma_{\rm beam} + \Gamma_{\rm cell} + \Gamma_{\nabla B} = 1/30\,\text{hours} + 1/50\,\text{hours} + 1/100\,\text{hours} = 1/16\,\text{hours}\ . \qquad (12)$$

Thus, according to Eq. 9, the target polarization cannot be expected to exceed

$$P_{\rm max} = \frac{\gamma_{\rm SE}}{\gamma_{\rm SE} + \Gamma} = 0.66\ . \qquad (13)$$

Realistically, we will not achieve a Rb polarization of 100% in the pumping chamber, which will reduce the polarization to about 45–50%.

V.2 Target Cells

The construction and filling of the target cells must be accomplished with great care if $1/\Gamma_{\rm cell}$ is to be in excess of 50 hours. We plan to use the "Princeton Prescription" which was developed for use in SLAC E-142. This resulted, among the cells that were tested, in lifetimes that were always better than 30 hours, and in about 60% of the cells, better than 50 hours. The following precautions will be taken:

- 1. Cells will be constructed from aluminosilicate glass.
- 2. All tubing will be "resized." This is a process in which the diameter of the tubing is enlarged by roughly a factor of two in order to insure a smooth pristine glass surface that is free of chemical impurities.
- 3. Cells will be subjected to a long (4–7 day) bake-out at high ($> 400^\circ$C) temperature on a high vacuum system before filling.
- 4. Rb will be doubly distilled in such a manner as to avoid introducing any contaminants to the system.

- 5. The ^{3}He will be purified either by getters or a liquid ^{4}He trap during filling.

The cells will be filled to a high density of ^{3}He by maintaining the cell at a temperature of about 20 K during the filling process. This is necessary so that the *pressure* in the cell is below one atmosphere when the glass tube through which the cell is filled is sealed.

The length of the cell has been chosen to be 40 cm and the end windows themselves will be about 100 μ thick. Thinner windows could in principle be used, but this does not appear to be necessary since they will not be directly seen by the spectrometer acceptance.

V.3 The Optics System

As mentioned above, approximately 20–24 Watts of "usable" light at 795 nm will be required. By "usable," we essentially mean light that can be readily absorbed by the Rb. It should be noted that the absorption line of the Rb will have a full width of several hundred GHz at the high pressures of ^{3}He at which we will operate. Furthermore, since we will operate with very high Rb number densities that are optically quite thick, quite a bit of light that is not within the absorption linewidth is still absorbed.

It is our plan to take advantage of new emerging diode laser technology to economically pump the target. Systems are now commercially available in which a single chip produces about 20 watts of light, about half of which is probably usable. Between 2–4 such systems should do the job. There is also a group at Lawrence Livermore Laboratory that has offered to build a single chip that can produce 150 watts. While some studies of the use of diode lasers for spin-exchange optical pumping do exist in the literature [38], actual demonstrations of high polarizations in cells suitable for targets are much more recent [39]. It is our opinion that diode lasers will probably work, but we will perform several tests before freezing this decision.

At SLAC, five titanium-sapphire/argon ion laser systems were used to drive the E-142 polarized ^{3}He target. This option will definitely work if the diode lasers are not sufficient.

V.4 Polarimetry

Polarimetry will be accomplished by two means. During the experiment, polarization will be monitored using the NMR technique of adiabatic fast passage (AFP) [40]. The signals will be calibrated by comparing the ^{3}He NMR signals with those of water. The calibration will be independently verified by studying the frequency shifts that the polarized ^{3}He nuclei cause on the electron paramagnetic resonance (EPR) lines of Rb atoms [35]. This second technique will be performed in separate target studies, not during the experiment. It will serve solely as a check of our calibration. We plan to determine the polarization of the target to an accuracy of 5%

V.5 Apparatus Overview

The target will be in air or, perhaps, in a helium bag. This greatly simplifies the design. The main components of the target are shown in Fig. 6.

The "main coils" shown are large Helmholtz coils that will be used to apply a static magnetic field of about 20 Gauss. In addition to establishing the quantization axis for the target, the main coils are important for suppressing relaxation due to magnetic field inhomogeneities, which go like $1/B^2$. At 20 G, inhomogeneities can be as large as about 30 mG/cm while keeping $\Gamma_{\nabla B} < 1/100$ hours. By increasing the applied field to about 40 G, and relaxing our requirements on $\Gamma_{\nabla B}$ by about factor of two, inhomogeneities as large as 0.25 G/cm can be tolerated. We are still finalizing our final choice of static field.

The NMR components in the target include a set of RF drive coils, and a separate set of pick-up coils. Not shown in the figure are the NMR electronics, which include an RF power amplifier, a lock-in amplifier, some bridge circuitry, and the capability to sweep the static magnetic field.

The oven shown in Fig. 6 is constructed of Torlon, a high temperature plastic. The oven is heated with forced hot air.

The laser system will consist of 2–4 laser diode systems. There will also be several lenses and a quarter wave plate to provide circular polarization.

VI. Contribution of the Collaboration and Beam Time Request

Contribution of the collaboration:

- Construction and installation of the polarized ^{3}He target.

We request from Jefferson Lab:

- Polarized beam up to 15μA with a beam polarization of 80% at energies of 4 and 6 GeV.
- Support for target installation in Hall A. However if this experiment runs immediately after an already scheduled Hall A ^{3}He experiment, the target can be left in place for this experiment.
- Working polarimeter to measure beam polarization.

We request a total running time of 680 hours to perform the complete experiment. 600 hours will be used for production running (assuming 100% running efficiency), about 30 hours for polarization measurements (about 1 hour per day), and 50 hours for background studies.

References

[1] E80 Collaboration, M.J. Alguard *et al.*, *Phys. Rev. Lett.* **37**, 1261 (1976); E80 Collaboration, M.J. Alguard *et al.*, *Phys. Rev. Lett.* **41**, 70 (1978).

[2] E130 Collaboration, G. Baum *et al.*, *Phys. Rev. Lett.* **51**, 115 (1983).

[3] EMC Collaboration, J. Ashman *et al.*, *Phys. Lett.* B **206**, 364 (1988); J. Ashman *et al.*, *Nucl. Phys.* B **328**, 1 (1989).

[4] E142 Collaboration, P.L Anthony *et al.*, *Phys. Rev. Lett.* **71**, 959 (1993).

[5] E143 Collaboration, K. Abe *et al.*, *Phys. Rev. Lett.* **74**, 346 (1994).

[6] SMC Collaboration, B. Adeva *et al.*, *Phys. Lett.* B **302**, 533 (1993).

[7] HERMES Collaboration, K. Ackerstaff *et al.*, *Phys. Lett.* B **404**, 383 (1997)

[8] E154 Collaboration, K. Abe *et al.*, *Phys. Rev. Lett.* **79**, 26 (1997).

[9] S. Wandzura and F. Wilczek, *Phys. Lett.* B **72**, 195 (1977).

[10] R.L. Jaffe and X. Ji, *Phys. Rev.* D **43**, 724 (1991).

[11] R.L. Jaffe, *Comments Nucl. Part. Phys*, Vol. 19, 239 (1990).

[12] P. Anthony *et al.*, *Phys. Rev.* D **54**, 6620 (1996).

[13] K. Abe *et al.*, *Phys. Rev. Lett.* **76**, 587 (1996).

[14] K. Abe *et al.*, *Phys. Lett.* B **404**, 377 (1997).

[15] Experiment 94-010 at TJNAF, "Measurement of the Neutron (^{3}He) Spin Structure Function at low Q^2; a Connection Between the BJ and DHG Sum Rules", spokespersons: G. Cates, Z.-E. Meziani; Experiment 95-001 at TJNAF, "Precise Measurements of the Inclusive Spin-dependent Quasi-elastic Transverse Asymmetry $A_{T'}$ from $^3\vec{\mathrm{He}}(\vec{e}, e')$ at Low Q^2, spokesperson: H. Gao.

[16] J. Qiu, private communication.

[17] M. Luo, J. Qiu, and G. Sterman, *Phys. Rev.* D **49**, 4493 (1994).

[18] E155x Collaboration, Proposal to Measure the Transverse Spin Structure Functions of the Proton and Deuteron at SLAC, (1997).

[19] M. Stratmann, ZPC **60**, 763 (1993).

[20] X. Song, *Phys. Rev.* D **54**, 1955 (1996).

[21] L.W. Whitlow *et al.*, *Phys. Lett.* B **250**, 193 (1990).

[22] NMC Collaboration,P. Amaudruz *et al.*, *Phys. Lett.* B **295**, 159 (1992).

[23] P. Bosted, E143 Technical Note 19, private communication.

[24] Review of Particle Properties, *Phys. Rev.* D **54**, 182 (1996).

[25] M. Stratmann, private communication.

[26] X. Song, private communication.

[27] K. Abe et al., E154-Collaboration, hep-ph/9705344.

[28] I.V. Akushevich and N.M. Shumeiko, J. Phys. G **20**, 513, (1994).

[29] M.A. Bouchiat, T.R. Carver and C.M. Varnum, *Phys. Rev. Lett.* **5**, 373 (1960).

[30] N.D. Bhaskar, W. Happer, and T. McClelland, *Phys. Rev. Lett.* **49**, 25 (1982).

[31] W. Happer, E. Miron, S. Schaefer, D. Schreiber, W.A. van Wijngaarden, and X. Zeng, *Phys. Rev.* A **29**, 3092 (1984).

[32] T.E. Chupp, M.E. Wagshul, K.P. Coulter, A.B. McDonald, and W. Happer, *Phys. Rev.* C **36**, 2244 (1987).

[33] K.P. Coulter, A.B. McDonald, W. Happer, T. E. Chupp, and M.E. Wagshul, *Nucl. Instrum. Methods* A **270**, 90 (1988).

[34] N.R. Newbury, A.S. Barton, P. Bogorad, G. D. Cates, M. Gatzke, H. Mabuchi, and B. Saam, *Phys. Rev.* A **48**, 558 (1993).

[35] K.P. Coulter, A.B. McDonald, G.D. Cates, W. Happer, T.E. Chupp, *Nucl. Instrum. Methods* A **276**, 29 (1989).

[36] N. R. Newbury, A. S. Barton, G. D. Cates, W. Happer, and H. Middleton, *Phys. Rev.* A **48**, 4411 (1993).

[37] G.D. Cates, S.R. Schaefer and W. Happer, *Phys. Rev.* A **37**, 2877 (1988); G.D. Cates, D.J. White, Ting-Ray Chien, S.R. Schaefer and W. Happer, *Phys. Rev.* A **38**, 5092 (1988).

[38] M. E. Wagshul and T. E. Chupp, *Phys. Rev.* A **40**, 4447 (1989).

[39] B. Cummings, private communication.

[40] A. Abragam, Principles of Nuclear Magnetism (Oxford University Press, New York, 1961).